Journal of Fluids and Structures 82 (2018) 173–197

Contents lists available at ScienceDirect

Journal of Fluids and Structures

journal homepage: www.elsevier.com/locate/jfs

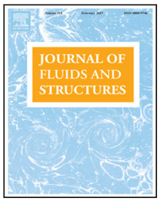

Aerodynamic damping of an oscillating fan blade: Mesh-based and meshless fluid structure interaction analysis

Christian D. Peters [a,*], Sybrand J. van der Spuy [a], Daniel N.J. Els [a], Jörg Kuhnert [b]

[a] *Stellenbosch University, Department of Mechanical and Mechatronic Engineering, Private Bag X1, Matieland 7602, South Africa*
[b] *Fraunhofer-Institut für Techno- und Wirtschaftsmathematik, Fraunhofer-Platz 1, 67663 Kaiserslautern, Germany*

ARTICLE INFO

Article history:
Received 24 October 2017
Received in revised form 22 May 2018
Accepted 6 July 2018

Keywords:
Two-way fluid structure interaction
Aeroelasticity
Turbulence modelling
Detached eddy simulation
Leading edge vortex
Meshless
Finite pointset method

ABSTRACT

An investigation is performed to determine the dynamic flow phenomena that dampen a fan blade's oscillation amplitude using numerical fluid structure interaction (FSI) simulations. Both a mesh-based and meshless numerical model are used to perform the FSI simulation and are compared according to their accuracy, robustness and computational cost. The meshless FSI simulation is performed by coupling the Finite Pointset Method (FPM) with a simplified 1D beam model. Experimental results from a separate investigation are used to validate the two numerical models.

This paper shows that both numerical models are suitable for modelling the aerodynamic damping of an axial fan used in an air cooled condenser fan unit. The observed flow effects include the formation and shedding of leading edge vortices, downwash, tip vortices and the added mass effect. Leading edge vortices are a major damping contributor and are found to mainly depend on the blade's effective angle of attack. The mesh-based and meshless FSI simulations are able to predict the experimentally determined tip displacement within an accuracy of 13% for 5 out of 6 simulations.

1. Introduction

Persistent water shortages in South Africa make the use of air cooled condensers (ACC) attractive. However, heat transfer is inhibited as the thermal conductivity and density of air are lower than that of water. To compensate for that, larger heat transfer surfaces and higher flow rates are employed in dry cooled condensers. The ACC at the Matimba power plant consists of 288 fan units with fan diameters of 9.13 m to handle its enormous cooling load, which can be more than 40 % of the heat input for fossil-fuel powered power plants (Kröger, 2004).

The arrangement of the fan units is depicted in Fig. 1. Neighbouring fan units and environmental factors, such as wind and air temperature, can significantly alter the flow conditions and distort the flow pattern within each fan unit. This not only leads to constantly varying condenser efficiencies, but also induces varying stresses in the different components of the ACC, which can lead to fatigue and may result in component failure.

The relationship between fan blade stresses and the axial air flow rate through the ACC fan unit was investigated by Muiyser et al. (2014). His findings show that the dominant vibration of the fan blade is caused by the fan blades' varying aerodynamic loading and occurs at approximately three times its rotational speed, which is its own natural frequency. Furthermore, his findings indicate that a higher axial flow velocity through the fan actually reduces the variation in flapwise bending loads of the fan blades. This suggests that the fan blade's vibrational motion is possibly damped due to the increased air flow rate through the fan. Such a phenomenon is termed aerodynamic damping and forms the focus of this research.

---

[*] Corresponding author.

https://doi.org/10.1016/j.jfluidstructs.2018.07.010
0889-9746/© 2018 Elsevier Ltd. All rights reserved.

Nomenclature

C_L	Lift coefficient
D_{Bl}	Blade displacement
D_P	Peak tip displacement
D_T	Tip displacement
E	Young's Modulus
f_V	Natural frequency in vacuum
f_{Max}	Frequency of highest order mode
h_{SL}	Smoothing length
k_{Bl}	Blade stiffness
L_{Bl}	Blade length
m_{AM}	Added mass
m_{Bl}	Blade mass
P_i	All points in the support domain of point i
r	Frequency ratio
r_P	Peak frequency ratio
t	Time variable
t_1 , t_2 , t_3 , t_4	Time instances in the blade's oscillation cycle as shown in Fig. 11
U	Velocity
U_{Bl}	Blade velocity
U_{In}	Inlet velocity
y^+	Dimensionless wall distance
z	Spanwise spatial variable
α	Angle of attack
α_E	Effective angle of attack
α_G	Geometric angle of attack
α_{ST}	Separation threshold angle of attack
Δt	Time step
Δt_{FEM}	Structural solver time step
Δt_{Max}	Maximum allowable time step
Δx	Cell length
δ	Amplitude decay factor
μ	Dynamic viscosity
ν	Poisson's ratio
$\omega_{d,Air}$	Angular damped natural frequency in air
ρ	Density
ζ_V	Damping coefficient in vacuum
ζ_a	Amplitude decay coefficient

Vectors and matrices

$\boldsymbol{C}$	Damping matrix
$\boldsymbol{D}$	Nodal degree of freedom vector
$\boldsymbol{D}_{Ext}$	Extrapolated nodal degree of freedom vector
$\dot{\boldsymbol{D}}$	Nodal degree of freedom velocity vector
$\ddot{\boldsymbol{D}}$	Nodal degree of freedom acceleration vector
$\boldsymbol{K}$	Stiffness matrix
$\boldsymbol{M}$	Mass matrix
$\vec{x}_{P,i}$	Position vector of point i

Abbreviations

ACC	Air cooled condenser
AFS	Against free stream
AOA	Angle of attack
BC	Boundary condition
CFL	Courant–Friedrich–Lewys
DES	Detached eddy simulation
FPM	Finite Pointset Method
FSI	Fluid structure interaction